NANOSYSTEMS: PHYSICS, CHEMISTRY, MATHEMATICS, 2019, 10 (6), P. 637–641

Pt nanoparticle-functionalized RGO counter electrode for efficient dye-sensitized solar cells

O. V. Alexeeva, S. S. Kozlov, L. L. Larina, O. I. Shevaleevskiy

Department of Solar Photovoltaics, Institute of Biochemical Physics RAS, Kosygin St. 4, Moscow, 119334, Russia
shevale2006@yahoo.com

PACS 73.63.Bd **DOI 10.17586/2220-8054-2019-10-6-637-641**

In this paper, we present a facile method for replacing conventional Pt-based counter electrode (CE) in dye-sensitized solar cells (DSCs) for the alternative low-cost nanostructured material containing reduced graphene oxide (RGO). Pt-NPs/RGO-based nanohybrid layers were synthesized at low temperature on a conductive glass substrate using microwave-assisted heating reduction strategy. The obtained material was characterized using XRD, SEM and TEM measurements and used for fabrication layered CEs on glass substrates. Photovoltaic characteristics of the DSCs based on Pt nanoparticle-functionalized RGO CEs were investigated under simulated AM1.5G solar illumination at an intensity of 1000 W/m^2. The obtained results have shown that Pt-NPs decorated RGO surfaces can be successfully used as CEs in high-efficiency DSCs and may be promising as low-cost electrodes in energy storage devices.

Keywords: nanostructures, reduced graphene oxide, thin films, semiconductors, solar photovoltaics, dye-sensitized solar cells.

Received: 1 December 2019

Revised: 4 December 2019

1. Introduction

In last few decades, dye-sensitized solar cells (DSCs), which reached over 12% power conversion efficiency, have attracted much attention as low cost alternatives to the conventional Si-based solid state solar cells (SCs) [1–3]. The main components of DSCs comprise a dye-sensitized mesoporous working photoelectrode (PE), redox electrolyte, and a counter electrode (CE) which plays a critical role in the reduction process of the dye-sensitized electrochemical cell processing.

Most studies so far have been focused on matching the device absorption characteristics to solar spectrum and the enhancement of the light collection ability of DSCs by the use of tandem systems, quantum dots, and new type of dyes [4–6]. However, much efforts have been also devoted in developing a new generation of more effective and low-cost PEs and CEs. Normally DSCs contain PEs based on a thin mesoscopic nanocrystalline titanium dioxide (TiO_2) layer with a bandgap (E_g) of around 3 eV. Recently, it was shown that zirconia dioxide (ZrO_2) with a very wide band-gap (E_g ~5.7 eV) can be also successfully used as a PE in DSCs and perovskite SCs with an ability to reduce the recombination effects at the interface between photoactive layer and working electrode [7–9].

The conversion efficiency of DSCs is critically dependent on the CE materials and a number of factors including electrical conductivity and catalytic activity [10]. In DSCs platinum-based (Pt-based) CEs have been widely used as the catalyst due to its good conductivity, high chemical stability and outstanding catalytic property. However, the conventional Pt layers on the flat FTO glass surface sputtered from expensive Pt targets demonstrate poor charge exchange ability and possess limited surface area for redox reactions [11]. Thus, there is a strong need in development of the alternative materials for replacing expensive Pt in high performance DSCs.

Graphenes and reduced graphene oxide (RGO) produced by reduction of graphene oxide (GO) have emerged promising low-cost counter electrode catalytic materials for high efficiency DSCs [12–15]. Interesting results were obtained when using CVD grown graphene and RGO for this purpose [16].

In more advanced approaches, CEs were fabricated by decorating tracing amounts of Pt nanoparticles (Pt-NPs) on RGOs (Pt-NPs/RGO) prepared using laser- and plasma-based reduction of GO and Pt-NPs precursors [12]. However, the requirements for a two-step process and high temperature of around 350 °C for plasma reduction may limit the practical realization of these methods. High-performance DSCs were fabricated using CEs based on RGO functionalized with large (100 nm) Pt nanoparticles (L-Pt/RGO) which were prepared at ambient temperatures using γ-ray irradiation [17].

In this study, nanometer-size Pt-NPs-decorated RGO (Pt-NPs/RGO) were prepared under low temperatures using a facile synthesis via a microwave irradiation assisted method and used as a catalyst material for constructing efficient CEs. The structure and morphologies of CEs were characterized using XRD, SEM and TEM measurements. Using the developed Pt-NPs/RGO CEs, we have fabricated DSCs and provided the measurements of the main photovoltaic parameters under AM1.5G solar illumination.

2. Experimental

2.1. Synthesis and characterization of Pt-NPs/RGO CEs

Graphene nanoplatelets (grade C-500, 500 m^2/g) were purchased from Sigma-Aldrich GmbH. Pt NPs on RGO sheets were sensitized using the procedure described in [18]. Graphene oxide (GO) was added into a solution of benzyl alcohol and sonicated for 60 min to obtain a homogenous liquid GO suspension. Microwave pulsed irradiation reactor operated under 2.45 GHz (Energiya-K-1-2450, Russia) was used for treating the solution for 3 min at 150 °C. After cooling and washing of the obtained suspension the synthesis of RGO was fulfilled by drying in vacuum during 10 h. To obtain liquid RGO suspension the obtained RGO was added to a solution of ethylene and sonicated for 60 min. H_2PtCl_6 was added to RGO suspension and stirred for 1 h. The obtained solution was then subjected to pulsed microwave heating for 3 min in a microwave reactor operated at 150 °C. After microwave irradiation, the suspension was cooled down to room temperature and the solid product was isolated, washed and dried for 12 h.

The structure and composition of Pt-NPs/RGO hybrid was analyzed by X-ray diffraction (XRD) spectroscopy using Regaku D/MAX-RC diffractometer. The morphology of Pt-NPs/RGO was investigated using field-emission scanning electronic microscope (FESEM; Hitachi S-4800) without a preliminary covering of the samples with any conductive coatings. High-resolution TEM (HRTEM) measurements were provided using a JEOL 2100F (Japan). For TEM measurements a drop of diluted in an ethanol Pt/RGO dispersion ($\sim$0.5 μl) was deposited on a carbon grid. Two different CEs were prepared for comparison. GO coated CE was fabricated following the known procedure [19]. Pt nanoparticles-decorated RGO counter electrodes were fabricated as described in [20].

2.2. Fabrication and characterization of DSCs

The details of the fabrication process of DSCs can be found on our previous publications [3, 6]. Briefly, TiO_2 nanostructured layer deposited onto FTO coated conductive glass substrate was used as a PE. To perform the sensitization a TiO_2 PE, the FTO-coated glass electrodes were dipped in a 0.3mM of N719 dye solution in a mixture of acetonitrile and tert-butyl alcohol (1:1 volume ratio) for 24 h. Then the dye-sensitized PE was rinsed with ethanol to remove the residues and dried at room temperature. Finally, the counter and photo electrodes were assembled into a sandwich-type cell and sealed with ionomer film (Surlyn 1702). The commercially available 1,2-Dimethyl-3-propylimidazolium iodide electrolyte AN-50 (Solaronix) was used to fulfill the fabrication of a photovoltaic device. The active area of the fabricated DSCs was around 0.11 cm^2.

The measurements of the photovoltaic parameters of the DSCs were provided under simulated AM1.5G solar illumination with intensity P_{IN} = 1000 W/m^2. The current voltage characteristics (J–V) were recorded using Keithley 4200-SCS Parameter Analyzer (USA) and Abet Technologies Solar Simulator (Abet, USA) as a light source. The power conversion efficiency (η) of the DSC was calculated from the J–V data using the known formula:

$$\eta = \frac{J_{SC} V_{OC} FF}{P_{IN}} \times 100\%$$

where J_{SC} – short-circuit current density, V_{OC} – open-circuit voltage, FF – fill factor and P_{IN} – light intensity of solar radiation.

3. Results and discussion

The formation of Pt-NPs on RGO structures was confirmed by XRD. Fig. 1 shows XRD patterns of the Pt-NPs/RGO layer on a glass substrate. The broad diffraction peaks at around $2\theta = 39.8°$ and $46.2°$ match perfectly with the (111) and (200) crystalline planes respectively for the face centered Pt cubic structure.

High resolution scanning electron microscope (HRSEM) images of RGO and Pt-NPs/RGO CE structures are shown in Fig. 2. HRSEM plane images of RGO nanoplatelets (Fig. 2a) show that the RGO flakes are randomly and closely distributed with each other in a condensed layer. The surface morphology of CEs (Pt-NPs/RGO) presented in Fig. 2b shows that Pt NPs are immobilized on the RGO surface with a high surface coverage and high loading of NPs. Graphene nanoplatelets are clearly visible in the micrographs. The structure of RGO layers seen in Fig. 2 possesses high surface area and mesoporous-like volume structure which is favorable for the penetration of electrolyte ions thus improving the electrochemical catalytic activity of CE in DSCs.

The morphology of Pt-NPs immobilized on RGO surface as analyzed by HRTEM in different magnifications is presented in Fig. 3. It is seen that Pt nanoparticles with an average size of 30 nm are well attached to RGO nanoplatelets that suggests a perfect interaction between the functional groups of RGO and Pt nanoparticles.

Figure 4 shows a comparative view of the I–V curves recorded for the DSCs fabricated with Pt-NPs/RGO CE and with GO CE. Previously it was confirmed that the DSC performance is strongly affected by the CE parameters such as electrical conductivity and electrochemical catalytic activity for the iodide/triiodide redox couple [18]. PV

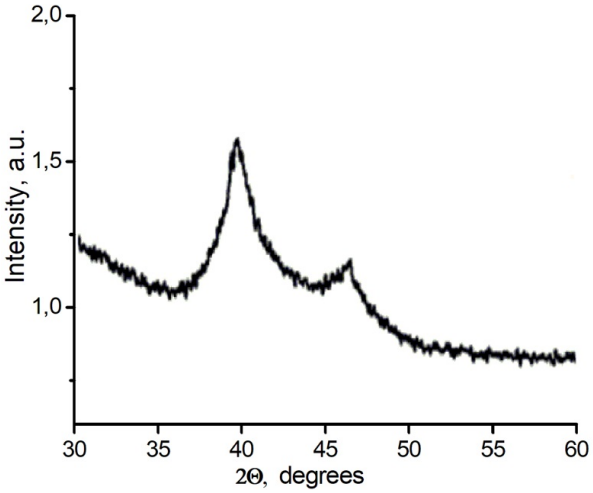

FIG. 1. XRD patterns of Pt-NPs/RGO composite

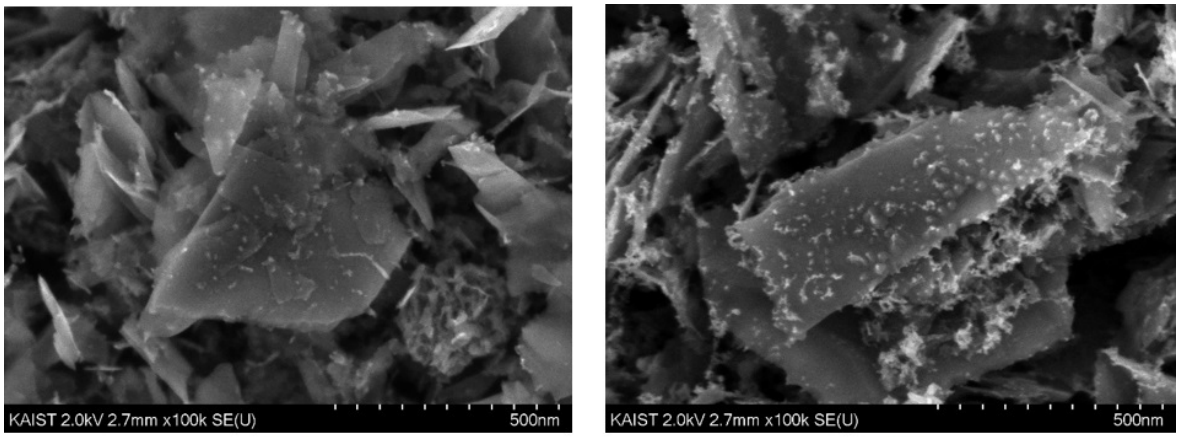

FIG. 2. HRSEM plane images of CE surface: (a) RGO nanoplatelets; (b) Pt-NPs immobilized on the RGO surface (Pt-NPs/RGO CE)

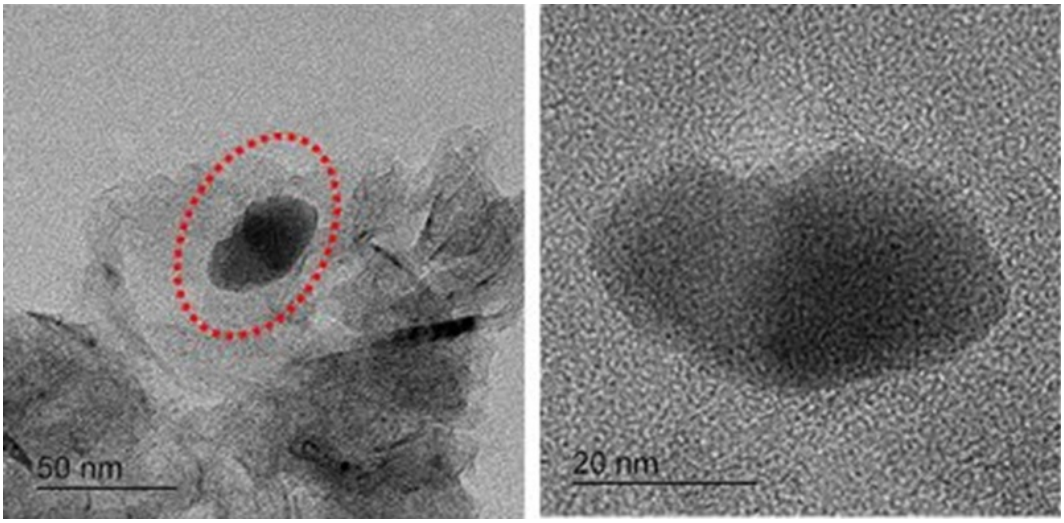

FIG. 3. Different magnification HRTEM images of Pt-NPs immobilized on RGO surface

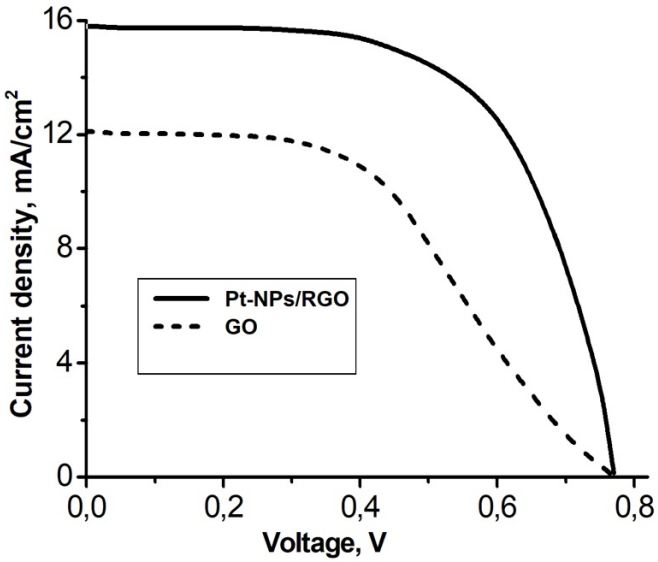

FIG. 4. J-V characteristics of DSCs with different CEs under simulated AM 1.5G solar illumination

measurements of the main DSC parameters clearly show the advantages of the Pt-NPs/RGO nanohybrids to provide perfect electrochemical catalytic activity when using as a CE in a photo electrochemical device. Fig. 4 shows that the DSC fabricated with Pt-NPs-decorated RGO counter electrode delivered the efficiency of 7.29% with $J_{SC} = 15.7$ mA/cm^2, $FF = 65.4$, and $V_{OC} = 0.71$ V. The alternative DSC configuration fabricated with a totally Pt-free GO CE has much poor performance and possesses non-typical I-V curve behavior. DSC based on GO counter electrode has shown the efficiency of 3.4% with $J_{SC} = 12.1$ mA/cm^2, $FF = 39.8$, and $V_{OC} = 0.7$ V. It should be noted that FF value in DSC based on GO CE was found to be nearly twice less than that obtained for Pt-NPs/RGO CE. As a result, the power conversion efficiency of the GO-based DSC was much decreased. We may propose that the observed poor behavior of the FF parameter may arise from factors including the poor catalytic activity of the GO electrode and high sheet resistance of the GO layer.

4. Conclusions

In summary, Pt-NPs/RGO-based nanohybrid layers were successfully synthesized at low temperature on a conductive glass substrate using microwave-assisted heating reduction method. SEM and TEM results have shown Pt NPs with a size of around 10 nm uniformly dispersed on the RGO surfaces. Pt-NPs/RGO-based layers were used as CEs for DSCs fabrication. The photovoltaic parameters of DSCs with nanohybrid CEs were achieved under simulated AM1.5G solar illumination and have shown long-term stability and high energy conversion performance of DSCs. The performance of 7.29%, with $J_{SC} = 15.7$ mA/cm^2, $FF = 65.4$, and $V_{OC} = 0.71$ V, was achieved for DSC fabricated with Pt-NPs-decorated RGO counter electrode. Thus, it was confirmed that small amounts of Pt nanoparticles decorated on RGO surfaces can be successfully used in low-cost electrodes for solar cells and energy storage devices such as lithium batteries and supercapacitors.

Acknowledgment

This research was supported by RFBR grant 16-29-06416.

References

[1] O'Regan B., Gratzel M. A low-cost, high-efficiency solar cell based on dye-sensitized colloidal TiO_2 films. *Nature*, 1991, **353**, P. 737–740.
[2] Shevaleevskiy O. The future of solar photovoltaics: from physics to chemistry. *Pure Appl. Chem.*, 2008, **80**, P. 2079–2089.
[3] Nikolay T., Larina, L., Shevaleevskiy O., Ahn B.T. Electronic structure study of lightly Nb-doped TiO_2 electrode for dye-sensitized solar cells. *Energ. Environ. Sci.*, 2011, **4**, P.1480–1486.
[4] Vildanova M.F., Nikolskaia A.B., Kozlov S.S., Shevaleevskiy O.I., Larina L.L. Novel types of dye-sensitized and perovskite-based tandem solar cells with a common counter electrode. *Tech. Phys. Lett.*, 2018, **44**(2), P. 126–129.
[5] Yum J., Jung I., Baik. C., Ko J., Nazeeruddin M.K., Gratzel M. High efficient donor–acceptor ruthenium complex for dye-sensitized solar cell application. *Energ. Environ. Sci.* 2009, **2**, P. 100–102.
[6] Dao V.D., Choi Y., Yong K., Larina L.L., Shevaleevskiy O., Choi H.-S. A facile synthesis of bimetallic AuPt nanoparticles as a new transparent counter electrode for quantum-dot-sensitized solar cells. *J. Power Sources*, 2015, **274**, P. 831–838.

[7] Larina L.L., Alexeeva O.V., Almjasheva O.V., Gusarov V.V., Kozlov S.S., Nikolskaia A.B., Vildanova M.F., Shevaleevskiy O.I. Very wide-bandgap nanostructured metal oxide materials for perovskite solar cells. *Nanosystems: Phys. Chem. Math.*, 2019, **10**(1), P. 70–75.

[8] Almjasheva O.V., Smirnov A.V., Fedorov B.A., Tomkovich M.V., Gusarov V.V. Structural features of ZrO_2–Y_2O_3 and ZrO_2–Gd_2O_3 nanoparticles formed under hydrothermal conditions. *Russ. J. Gen. Chem.*, 2014, **84**(5), P. 804–809.

[9] Bugrov A.N., Almjasheva O.V. Effect of hydrothermal synthesis conditions on the morphology of ZrO_2 nanoparticles. *Nanosystems: Phys. Chem. Math.*, 2013, **4**, P. 810–815.

[10] Kannan A.G., Zhao J., Jo S.G., Kang Y.S., Kim D.-W. Nitrogen and sulfur co-doped graphene counter electrodes with synergistically enhanced performance for dye-sensitized solar cells. *J. Mater. Chem.* A, 2014, **2**, P. 12232–12239.

[11] Somik M., Balavinayagam R., Griggs L., Hamm S., Baker G.A., Fraundorf P., Sengupta S., Gangopadhyay S. Ultrafine sputter-deposited Pt nanoparticles for triiodide reduction in dye-sensitized solar cells: impact of nanoparticle size, crystallinity and surface coverage on catalytic activity. *Nanotechnology*, 2012, **23**, P. 485405.

[12] Dao V.-D., Hoa N.T.Q., Larina L.L., Lee J.-K., Choi H.-S. Graphene-platinum nanohybrid as a robust and low-cost counter electrode for dye-sensitized solar cells. *Nanoscale*, 2013, **5**, P. 12237–12244.

[13] Chen J., Yao B., Li C., Shi G. An improved Hummers method for eco-friendly synthesis of graphene oxide. *Carbon*, 2013, **64**, P. 225–229.

[14] Gong F., Wang H., Wang Z.-S., Self-assembled monolayer of graphene/Pt as counter electrode for efficient dye-sensitized solar cell. *Phys. Chem. Chem. Phys.*, 2011, **13**, P. 17676–17682.

[15] Qui L., Zhang H., Wang W., Chen Y., Wang. R. Effects of Pt/RGO as counter electrode in dye-sensitized solar cells. *Appl. Surf. Sci.*, 2014, **319**, P. 339–343.

[16] Zhang D.W., Li X.D., Li H.B., Chen S., Sun Z., Yin X.J., Huang S.M. Graphene-based counter electrode for dye-sensitized solar cells. *Carbon*, 2011, **49**(15), P. 5382–5388.

[17] Ahn H.-J., Lee J.-S., Kim H.-S., Hwang I.-T., Hong J.-H., Shin J., Jung C.-H. Fabrication of large Pt nanoparticles-decorated rGO counter electrode for highly efficient DSSCs. *J. Ind, Eng. Chem.*, 2018, **65**, P. 318–324.

[18] Yoon S.-W., Dao V.-D., Larina L.L., Lee J.-K., Choi H.-S. Optimum strategy for designing PtCo alloy/reduced graphene oxide nanohybrid counter electrode for dye-sensitized solar cells. *Carbon*, 2016, **96**, P. 229–336.

[19] Dao V.-D., Ko S.H., Choi H.-S., Lee J.-K. Pt-NP–MWNT nanohybrid as a robust and low-cost counter electrode material for dye-sensitized solar cells. *J. Mater. Chem.*, 2012, **22**, P. 14023–14029.

[20] Dao V.-D., Tran C.Q., Ko S.-H., Choi H.-S. Dry plasma reduction to synthesize supported platinum nanoparticles for flexible dye-sensitized solar cells. *J. Mater. Chem. A*, 2013, **1**, P. 4436–4443.